

Interaction of Indolicidin with Model Lipid Bilayers: FTIR-ATR Spectroscopic Study

Mi Kyung Bahng, Nam Jeong Cho, Jong Sang Park, and Kwan Kim*

Department of Chemistry and Center for Molecular Catalysis, Seoul National University, Seoul 151-742, Korea

Received August 4, 1997. In Final Form: October 30, 1997[®]

An attempt has been made using Fourier transform infrared–attenuated total reflection (FTIR-ATR) spectroscopy to see the molecular level interaction between indolicidin, a tridecapeptide known to possess antimicrobial activity, and model phospholipid bilayers. Initially, model lipid bilayers were assembled on ZnSe plates with compounds of dipalmitoylphosphatidic acid (DPPA), dipalmitoylphosphatidylcholine (DPPC), and dipalmitoylphosphatidylglycerol (DPPG) using the Langmuir–Blodgett (LB) method. From the FTIR-ATR dichroic ratios measured with and without rotation of the ATR plates, the LB lipid bilayers seemed to be described in terms of a uniaxial orientational model. Along with a cyclic voltammetry measurement, the ATR spectra dictated that indolicidin molecules were readily incorporated inside the acyl chains of the lipid bilayers. Furthermore, from the infrared absorption frequencies of amide I bands, indolicidin molecules that consisted of ill-defined random-coil structures in an aqueous medium appeared to adopt a 3_{10} -helical conformation inside the lipid bilayers. This view was in good agreement with the electronic circular dichroism observed for PC (+10% cardiolipin) vesicles mixed with an indolicidin solution.

Introduction

Indolicidin, a tridecapeptide amide, was isolated by Selsted et al.¹ from the cytoplasmic granules of bovine neutrophils (its primary structure is H-Ile-Leu-Pro-Trp-Lys-Trp-Pro-Trp-Trp-Pro-Trp-Arg-Arg-NH₂). Named for its unusual abundance of tryptophan (38%), indolicidin is a structurally unique antimicrobial peptide. In this regard, much interest has been focused on its therapeutic utility. Indolicidin was found, however, to be highly toxic not only to bacterial cells but to mammalian cells as well. Nonetheless, Ahmad et al.² reported that liposomally encapsulated indolicidin had significantly reduced toxicity.

The biological activity of indolicidin has been studied extensively,^{3,4} but a detailed mechanism of the action of indolicidin is not yet clearly understood. Recently, referring to the circular dichroism (CD) spectra of indolicidin taken in the presence and the absence of 1-palmitoyl-2-oleoyl-*sn*-glycero-3-phosphocholine (POPC)/1-palmitoyl-2-oleoyl-*sn*-glycero-3-phosphoglycerol (POPG) (7:3) liposomes, Falla et al.⁵ suggested that indolicidin molecules assumed a poly-L-proline II helical structure when interacting with liposomes. On the other hand, Ladokhin et al.⁶ reported that indolicidin adopted a slightly ordered but not α -helical structure in SDS micelles.

Fourier transform infrared–attenuated total reflection (FTIR-ATR) spectroscopy has been regarded as a useful

means of studying the oriented layers of lipids, proteins, and lipid–protein composite systems assembled on an ATR element by either spin-coating or the Langmuir–Blodgett (LB) method.^{7–11} We have thus undertaken a FTIR-ATR spectroscopic study to see the possibility of molecular-level interaction between indolicidin and model phospholipid bilayers consisting of dipalmitoylphosphatidic acid (DPPA), dipalmitoylphosphatidylcholine (DPPC), and dipalmitoylphosphatidylglycerol (DPPG). To simplify the investigation, the model lipid single bilayers were prepared on hydrophilic ATR elements by a Y-type deposition LB method,⁸ and then the elements were placed in contact with an aqueous indolicidin solution. From the FTIR-ATR spectra recorded before and after contact, the effect of indolicidin on the phospholipid acyl chain ordering was examined along with the deduction of the conformational change of indolicidin upon interacting with the lipid bilayers. In order to help interpret the FTIR-ATR spectra, an electronic circular dichroism measurement was undertaken for PC (+10% cardiolipin) vesicles mixed with an indolicidin solution. Besides, a cyclic voltammetry measurement was performed at a Au electrode, coated with an octadecanethiolate/DPPA bilayer, to see the favorableness of transport of electroactive species through the bilayer before and after treating the coated electrode in indolicidin solution.

Experimental Section

Indolicidin was synthesized by solid-phase peptide synthesis (SPPS)⁴ using 9-fluorenylmethoxycarbonyl amino (Fmoc) acids and Rink amide resin from AnaSpec (San Jose, CA) and Nova Biochem (La Jolla, CA). Following synthesis, indolicidin was

* Author to whom all correspondence should be addressed. Telephone: 82-2-880-6651. Fax: 82-2-889-1568. E-mail: kwankim@plaza.snu.ac.kr.

[®] Abstract published in *Advance ACS Abstracts*, December 15, 1997.

(1) Selsted, M. E.; Novotny, M. J.; Morris, W. L.; Tang, Y. Q.; Smith, W.; Cullor, J. S. *J. Biol. Chem.* **1992**, *267*, 4292–4295.

(2) Ahmad, I.; Perkins, W. R.; Lupan, D. M.; Selsted, M. E.; Janoff, A. S. *Biochim. Biophys. Acta* **1995**, *1237*, 109–114.

(3) Aley, S. B.; Zimmerman, M.; Hetsko, M.; Selsted, M. E.; Gillin, F. D. *Infect. Immun.* **1994**, *62*, 5397–5403.

(4) Abel, R. J. V.; Tang, Y.; Rao, V. S. V.; Dobbs, C. H.; Tran, D.; Barany, G.; Selsted, M. E. *Int. J. Peptide Protein Res.* **1995**, *45*, 401–409.

(5) Falla, T. J.; Karunaratne, D. N.; Hancock, R. E. W. *J. Biol. Chem.* **1996**, *271*, 19298–19303.

(6) Ladokhin, A. S.; Selsted, M. E.; White, S. H. *Biophys. J.* **1997**, *72*, 794–805.

(7) Dluhy, R. A.; Cornell, D. G. In *Fourier Transform Infrared Spectroscopy in Colloid and Infection Science*; Scheuing, D. R., Ed.; American Chemical Society: Washington, DC, 1991.

(8) Swart, R. M. In *Langmuir-Blodgett Films*; Roberts, G., Ed.; Plenum Press, New York, 1990.

(9) Ball, A.; Jones, R. A. L. *Langmuir* **1995**, *11*, 3542–3548.

(10) Naydenova, S.; Petrov, A. G.; Yarwood, J. *Langmuir* **1995**, *11*, 3435–3437.

(11) Surewicz, W. K.; Mantsch, H. H.; Chapman, D. *Biochemistry* **1993**, *32*, 389–394.

cleaved from the resin, and protecting groups were removed by treatment with a solution containing 82.5% trifluoroacetic acid, 5% water, 5% phenol, 5% anisol, and 2.5% dithioethanol for 5 h at room temperature. Indolicidin was then precipitated in diethyl ether. A Vydac C18 reversed-phase high-performance liquid chromatography (HPLC) column (5 micron, 4.6×250 mm) was used to purify indolicidin using a 20%/100% water/acetonitrile gradient containing 0.1% trifluoroacetic acid. The identities and purities of indolicidin variants were confirmed by fast atom bombardment mass spectrometry (FABMS).

PC, cardiolipin, and synthetic phospholipids, that is, DPPA, DPPC, and DPPG, were all purchased from Sigma Chemical Co. and used as received. All chemicals unless specified were reagent grade, and triply distilled water (resistivity greater than $18.0 \text{ M}\Omega\cdot\text{cm}$) was used throughout.

To prepare lipid single bilayers on the ATR elements, a two-sided trapezoid ZnSe crystal ($52.5 \text{ mm} \times 20 \text{ mm} \times 2 \text{ mm}$) was immersed at 18°C into the subphase of water in the Langmuir trough (KSV Model 3000). Lipid (1 mg/mL in CHCl_3) was then spread on the air–water interface, and CHCl_3 was allowed to evaporate for 1 h. Subsequently, the lipid layer was compressed at a rate of 2 mm/min to a surface pressure of 30 mN/m . A Y-type deposition⁸ was employed to anchor lipid bilayers onto the hydrophilic ZnSe crystal by raising and lowering the crystal at the rates 2 and 70 mm/min , respectively (namely, in upstroke the head groups of lipid molecules interacted with the substrate surface, and thereafter in downstroke a second lipid monolayer was formed on the first monolayer by a hydrophobic interaction). The crystal was finally removed from the water subphase after the barrier of the Langmuir trough was fully expanded.

The lipid-bilayer-anchored ZnSe crystal was immersed in a $50 \mu\text{g/mL}$ indolicidin solution in water at 37°C for 20 min. After immersion, the crystal was rinsed thoroughly with water and then dried under a N_2 gas medium.

Cast films were also prepared with 10:1 or 30:1 (molar ratio) lipid/indolicidin mixtures. Initially, an aliquot amount of the mixture in 4:1 $\text{CHCl}_3/\text{MeOH}$ was spread on a ZnSe crystal and dried under N_2 atmosphere at room temperature. The crystal was further equilibrated with liquid water in order for the mixture to be in a liquid crystalline ultrastructure. The cast film was finally dried under a N_2 medium.

Infrared spectra of the above samples were obtained by using a Bruker IFS 113v FT-IR spectrometer equipped with a Specac ATR attachment, a Harrick wire-grid polarizer, and a liquid- N_2 -cooled mercury–cadmium–telluride detector. The incident angle of infrared light was set at 45° with respect to the plane of the ZnSe crystal such that 12 internal reflections in total took place throughout the crystal. The 128-times-scanned interferograms were collected at 4 cm^{-1} resolution, and their average was apodized with a Happ-Genzel apodization function.

Separately, circular dichroism (CD) measurement was performed for PC (+10% cardiolipin) vesicles mixed with indolicidin solution. To do this, PC and cardiolipin were initially mixed to obtain the desired ratio of negatively charged lipid. The solvent was removed by a stream of nitrogen, and a trace amount of chloroform was further removed by placing the lipid mixture in a freeze-dryer overnight. The lipid was resuspended in 50 mM phosphate buffer (pH 7.0) and then sonicated. When the vesicle was mixed with indolicidin solution, the final concentrations of PC and indolicidin were 2 mM and $18 \mu\text{M}$, respectively. The CD measurement was performed using a Jasco Model 720 spectropolarimeter equipped with a thermostat. Normally, 10 scans were recorded between 190 and 250 nm at 20°C with 0.1 cm path length. The data were not smoothed and were expressed in terms of $[\Theta]_T$, the total molar ellipticity ($\text{deg}\cdot\text{cm}^2\cdot\text{dmol}^{-1}$).

We have also carried out cyclic voltammetry (CV) measurements with a Au electrode covered with an octadecanethiolate/DPPA bilayer. To do this, initially, a Au (Aldrich, 99.99%) disk electrode (5 mm diameter) was immersed into a 5 mM octadecanethiol (ODT) solution in ethanol for 1 day. After the electrode was removed, it was rinsed with excess ethanol and then dried with a N_2 gas jet. Thereafter, a single DPPA layer was deposited onto the ODT layer by the LB method (via hydrophobic interaction). For CV measurements, a home-made three-electrode cell was used; an ODT/DPPA-coated Au electrode was used as a working electrode, a Pt wire was used as a counter electrode, and a

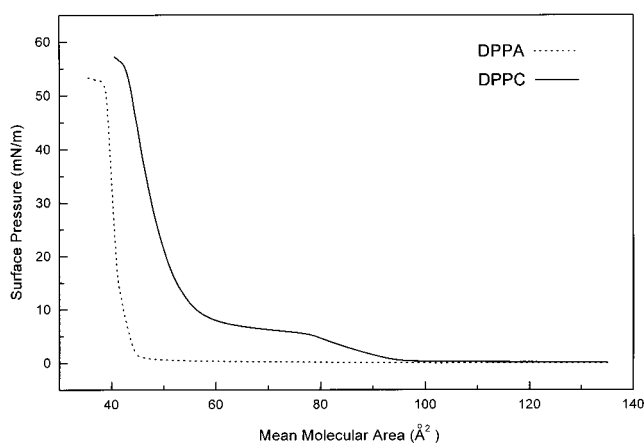


Figure 1. Surface Pressure–Area (π – A) Isotherm curves of DPPA and DPPC at the air–water interface at 18°C .

saturated calomel electrode (SCE) was used as a reference electrode. An aqueous solution of 1 M KCl was used as a supporting electrolyte. With a modified Au electrode, the CV response of 0.5 mM $\text{Fe}(\text{CN})_6^{3-}$ in solution was monitored at a scan rate of $40 \text{ mV}\cdot\text{s}^{-1}$ (prior to scanning, the solution was bubbled with nitrogen to reduce any dissolved oxygen). The same CV experiment was repeated after the ODT/DPPA coated Au electrode was soaked in a $50 \mu\text{g/mL}$ indolicidin solution in water at 37°C for a predetermined period of time. All the potentials are quoted versus a SCE.

Results and Discussion

Surface Pressure–Area Isotherms of DPPA and DPPC at the Air–Water Interface. Figure 1 shows the surface pressure–area (π – A) isotherm curves of pure DPPA and DPPC at the air–water interface at 18°C , respectively. Their features as well as the limiting surface areas, determined to be $42 (\pm 1) \text{ \AA}^2$ for DPPA and $53 (\pm 2) \text{ \AA}^2$ for DPPC, agree well with those reported in the literature.^{12–14}

ATR-IR Amide Bands of Indolicidin after Interaction with DPPA and DPPC Bilayers on ZnSe. Prior to presenting the ATR spectra of indolicidin, it would be worthwhile to recall that infrared spectra of proteins and peptides are usually characterized by the absorption bands of amide groups.^{15–18} The so-called amide I band is attributed to the combination of the $\text{C}=\text{O}$ (80%) and $\text{C}-\text{N}$ (10%) stretching vibrations and the in-plane $\text{N}-\text{H}$ bending (10%) vibration of peptide group(s). The amide II band has been claimed to be consisting of the in-plane $\text{N}-\text{H}$ bending (60%) and the $\text{C}-\text{N}$ stretching (40%) vibrations. When the amide group is involved in hydrogen bonding, the double-bond character of the $\text{C}-\text{N}$ bond increases and that of the $\text{C}=\text{O}$ bond decreases. This implies that the amide bands should be sensitive to the secondary structure of peptides. On the other hand, the capability of hydrogen–deuterium exchange in the amide group reflects the stability of peptides in conjunction with solvent exposure.¹⁸

Figure 2a shows the ATR spectrum of indolicidin dissolved in D_2O (this spectrum was taken with a nine-

(12) Lukes, P. J.; Petty, M. C.; Yarwood, J. *Langmuir* **1992**, *8*, 3043–3050.

(13) Solletti, J. M.; Botreau, M.; Sommer, F.; Brunat, W. L.; Kasas, S.; Duc, T. M.; Celio, M. R. *Langmuir* **1996**, *12*, 5379–5386.

(14) Essman, U.; Perera, L.; Berkowitz, M. L. *Langmuir* **1995**, *11*, 4519–4531.

(15) Miyazawa, T.; Shimanouchi, T.; Mizushima, S. *J. Chem. Phys.* **1958**, *29*, 611–616.

(16) Miyazawa, T. *J. Chem. Phys.* **1960**, *32*, 1647–1652.

(17) Kennedy, D. F.; Crisma, M.; Toniolo, C.; Chapman, D. *Biochemistry* **1991**, *30*, 6541–6548.

(18) Tu, A. T. In *Spectroscopy of Biological Systems*; Clark, R. J. H., Heister, R. E., Eds.; John Wiley & Sons Ltd.: New York, 1986.

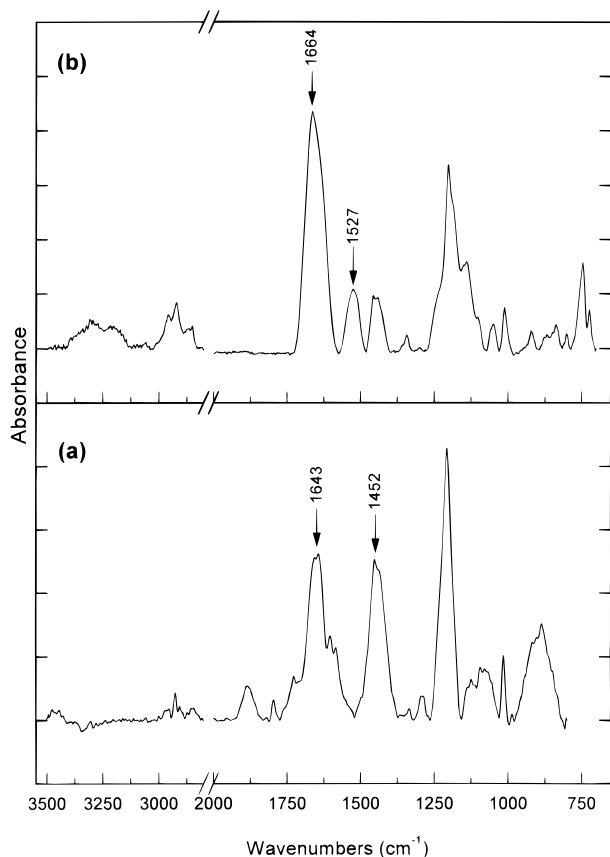


Figure 2. FTIR-ATR spectra of (a) indolicidin in D_2O (50 $\mu g/L$) and (b) indolicidin that is cast and dried on ZnSe. Before taking the latter spectrum, an aliquot amount of indolicidin in $CHCl_3$ was sprayed on a ZnSe crystal, and then the crystal was dried with a N_2 gas jet.

reflection ZnSe prism liquid cell). The spectrum exhibits the amide I band centered around 1643 cm^{-1} . The band can be attributed to the presence of indolicidin in an ill-defined random conformation. Figure 2b shows the ATR spectrum of neat indolicidin. To take the spectrum, an aliquot amount of indolicidin in $CHCl_3$ was sprayed on a ZnSe crystal, and then the crystal was dried with a N_2 gas jet. In Figure 2b, two distinct peaks are identified at 1664 (amide I) and 1527 (amide II) cm^{-1} . Referring to the literature data,^{19–21} these bands would be attributed to either a random coil or a 3_{10} -helical and/or distorted α -helical conformation. Nonetheless, as will be described later, it is suggested that they arise mainly from a 3_{10} -helical conformation. On the other hand, in Figure 2b one can notice also a shoulder peak at $\sim 1640\text{ cm}^{-1}$ (its position was determined from a second-derivative spectrum). This peak might be due to a small amount of water trapped inside the sample.²² However, considering that the sample was in a very dried state, the shoulder peak could be attributed alternatively to the amide I band of either a 3_{10} -helical¹⁷ or a β -turn¹⁷ structure and/or a β -sheet²¹ structure that is present under inter- and/or intramolecular hydrogen bonding. The amide bands of indolicidin identified in Figure 2 are summarized in Table 1.

Figure 3a shows the ATR spectrum of the DPPA bilayer, anchored on a ZnSe crystal by the LB method, in the 1400 –

Table 1. FTIR-ATR Spectral Data of Amide I and II Bands of Indolicidin

sample	amide I (cm^{-1})	amide II (cm^{-1})	assignments ^g
in D_2O ^a	1643 vs	1452 vs	random
cast on ZnSe ^b	1664 vs	1527 s	3_{10} -helix
	~ 1640 sh		3_{10} -helix/ β -turn/ β -sheet
inside LB/DPPA ^c	1664 vs	1527 s	3_{10} -helix
	~ 1640 sh		3_{10} -helix/ β -turn/ β -sheet
inside LB/DPPC ^d	1664 vs	1527 s	3_{10} -helix
	~ 1640 sh		3_{10} -helix/ β -turn/ β -sheet
cast with DPPA	1664 vs	1527 s	3_{10} -helix
	~ 1640 sh		3_{10} -helix/ β -turn/ β -sheet
cast with DPPC ^e	1687 vs	1520 vw	β -turn
	1664 sh		3_{10} -helix
	~ 1640 sh		3_{10} -helix/ β -turn/ β -sheet
cast with DOPC ^f	1687 vs	1520 vw	β -turn
	1664 sh		3_{10} -helix
	~ 1640 sh		3_{10} -helix/ β -turn/ β -sheet

^a See Figure 2a. ^b See Figure 2b. ^c See Figure 3b. ^d See Figure 3d. ^e See Figure 6a. ^f Figure 6b. ^g Shoulder peak at $\sim 1640\text{ cm}^{-1}$ may be due to a small amount of water trapped inside the sample. See text.

1800 cm^{-1} region (unless otherwise specified, all the ATR spectra shown in this work were taken with p-polarized light). Figure 3b represents the ATR spectrum taken after the crystal was immersed in indolicidin solution for 20 min and dried with a N_2 gas jet. It is seen that significant spectral change occurs upon placing the lipid bilayer in contact with indolicidin solution. When a clean ZnSe crystal is soaked in indolicidin solution, no peak is observed. This implies that indolicidin interacts readily with the DPPA bilayer. The peaks at 1664 and 1527 cm^{-1} in Figure 3b can be assigned, respectively, to the amide I and II bands of indolicidin incorporated in (or aggregated on) the DPPA bilayer. It is remarkable that their peak positions and band widths as well as their relative peak intensities are almost comparable to those in the ATR spectrum of neat indolicidin in the solid state (Figure 2b). A shoulder peak is also identified at $\sim 1640\text{ cm}^{-1}$ in Figure 3b. Hence, indolicidin molecules existing in aqueous medium with a random configuration are supposed to incorporate into (or aggregate onto) the DPPA bilayer and to adopt structure(s) similar to that of neat solid indolicidin. The amide bands of indolicidin identified in Figure 3 are also summarized in Table 1.

From the infrared spectral data alone, it is not evident whether indolicidin molecules penetrate into the DPPA bilayer or they simply aggregate on the bilayer with structure(s) similar to that of neat solid indolicidin. To resolve this difficulty, it was attempted to monitor the transport capability of an electroactive species, $Fe(CN)_6^{3-}$, through a lipid layer before and after immersion into indolicidin solution. As described in the Experimental Section, to mimic the DPPA single bilayers, an octadecanethiolate (ODT) monolayer was self-assembled initially on a 5-mm-diameter Au electrode (formation of close-packed ODT structure was confirmed not only by cyclic voltammetry (CV) but also by reflection-absorption infrared (RAIR) spectroscopy), and then a DPPA monolayer was anchored onto the ODT layer by the LB method (via hydrophobic interaction). Figure 4a shows the CV response of a bare gold electrode for $Fe(CN)_6^{3-}$ in 1 M KCl. Distinct cathodic and anodic peaks occurring from a reversible one-electron-transfer process are seen at 0.18 and 0.24 V versus SCE, respectively. Such peaks become completely absent when the Au electrode is covered with ODT (Figure 4b) and ODT/DPPA (Figure 4c) layers.

(19) Surewicz, W. K.; Mantsch, H. H. *Biochim. Biophys. Acta* **1988**, *952*, 115–130.

(20) Toniolo, C.; Crisma, M.; Bonora, G. M.; Benedetti, E.; Blasio, B. D.; Pavone, V.; Pedone, C.; Santini, A. *Biopolymers* **1991**, *31*, 129–138.

(21) Krimm, S.; Bandekar, J. *Adv. Protein Chem.* **1986**, *38*, 181–364.

(22) Marechal, Y.; Chamel, A. *J. Phys. Chem.* **1996**, *100*, 8551–8555.

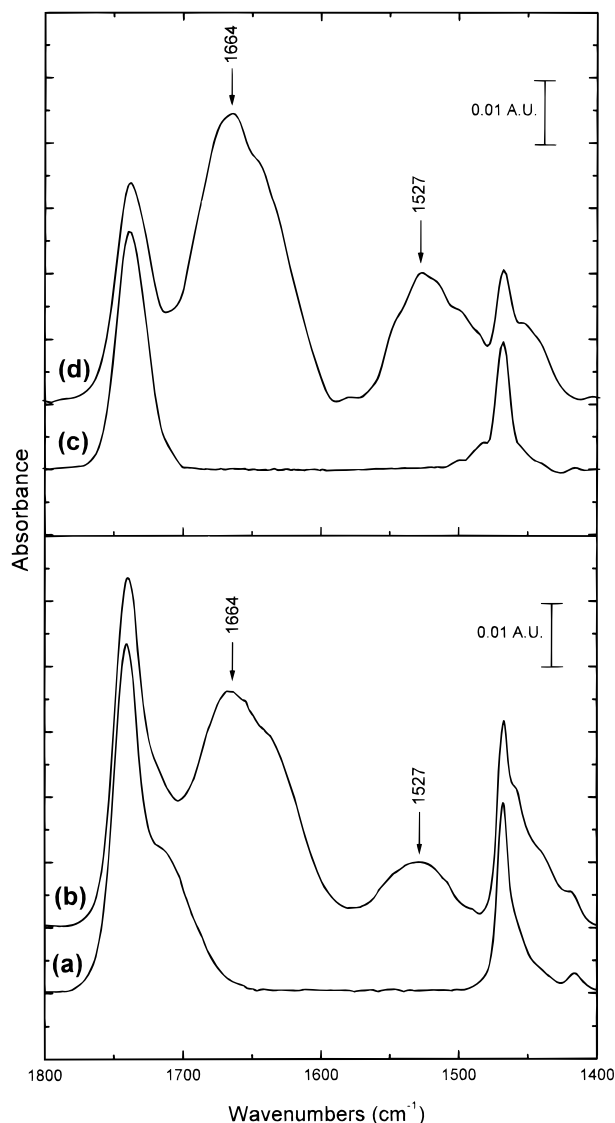


Figure 3. FTIR-ATR spectra in the 1400–1800 cm^{-1} region; LB films of DPPA bilayers on ZnSe (a) before and (b) after immersion in indolicidin solution (50 $\mu\text{g/mL}$) for 20 min, and LB films of DPPC bilayers on ZnSe (c) before and (d) after immersion in indolicidin (50 $\mu\text{g/mL}$) for 20 min.

However, as can be seen in Figure 4d, when a CV measurement was made after soaking the ODT/DPPA film in indolicidin solution for 15 min, cathodic and anodic peaks reemerged at 0.18 and 0.24 V, respectively, although their intensity was about one fifth of that observed at a bare Au electrode. This suggests that indolicidin molecules should penetrate deep into the ODT/DPPA layers. If indolicidin molecules were aggregated on the surface of the DPPA layer, CV peaks would not appear because the underlying ODT layer should still assume a close-packed structure.²³ It is also informative that the CV peaks become gradually weakened when the ODT/DPPA film is immersed for a more longer time. For instance, when a CV measurement is made after soaking the ODT/DPPA film in indolicidin solution for longer than 30 min, no CV peak is identified (see Figure 4e). In a separate RAIR spectroscopic study, it appeared that DPPA as well as ODT layers were left intact on a Au substrate even after a ODT/DPPA film on Au was immersed in indolicidin solution for several hours. Accordingly, it is supposed that indolicidin molecules penetrate into the lipid bilayers,

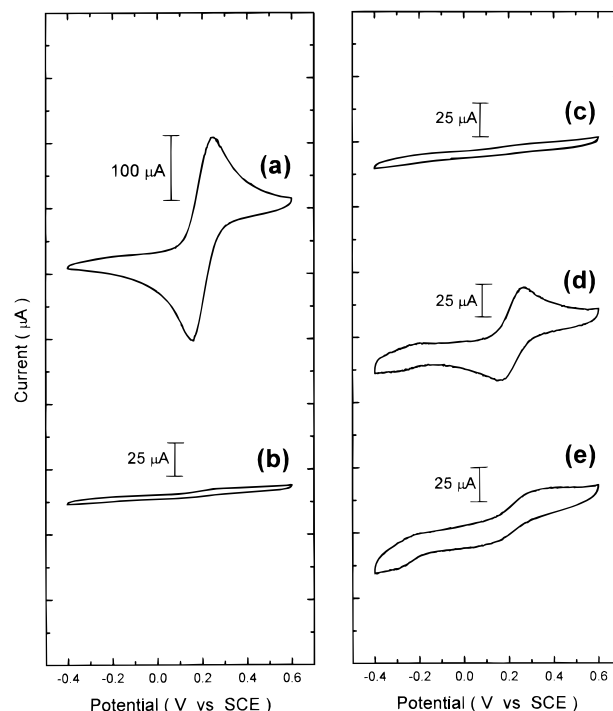


Figure 4. Cyclic voltammograms of 0.5 mM $\text{Fe}(\text{CN})_6^{3-}$ in 1 M KCl. Cyclic voltammograms carried out with (a) bare Au, (b) ODT-coated Au, and (c) ODT/DPPA-coated Au electrodes as working electrodes. The cyclic voltammograms shown in parts d and e were obtained with and ODT/DPPA-coated Au electrode after treating the electrode in a 50 $\mu\text{g/mL}$ indolicidin solution at 37 $^\circ\text{C}$ for 15 and 30 min, respectively. The scan rate was 40 $\text{mV}\cdot\text{s}^{-1}$. Potentials are versus a SCE.

and eventually they assemble along with the nearby lipid molecules into a rather close-packed structure such that the passage of electroactive species is through the film is not feasible. Similar CV observation has been reported in the literature for the $\text{Tl(I)}/\text{Tl(Hg)}$ couple at an electrode coated with gramicidine-modified lipid monolayers.²⁴

It has been well-documented²⁵ that peptides in random-coil structures are subjected to facile H/D exchange, and thereby the amide bands are red-shifted by more than 10 cm^{-1} . In this respect, it should be informative that even after the indolicidin-incorporated DPPA bilayer was immersed in D_2O for a prolonged time (>1 h), the amide I band was almost invariant, appearing at 1660 cm^{-1} , albeit the intensity of the amide II band became significantly weakened (by 90%). This indicates once again that the possibility of the presence of indolicidin with a random-coil structure is very low in the DPPA bilayer.

A strikingly similar ATR spectral observation was made for the DPPG and DPPC bilayers. Figure 3c shows the ATR spectrum of a DPPC bilayer anchored on a ZnSe crystal by the LB method. Figure 3d represents the ATR spectrum taken after the crystal was immersed in indolicidin solution for 20 min. The amide bands of indolicidin were clearly identified at 1664 and 1527 cm^{-1} . Their peak positions were barely different from those observed on the DPPA (Figure 3b) and DPPG bilayers. This suggests that indolicidin molecules should interact readily with even the DPPC bilayer, adopting a conformation similar to that in the DPPA bilayer. When the indolicidin-incorporated DPPC bilayer was immersed in D_2O , the amide band spectral feature was nearly invariant,

(24) Nelson, A. *Langmuir* **1996**, *12*, 2058–2067.

(25) Susi, H.; Timasheff, S. N.; Stevens, L. *J. Biol. Chem.* **1967**, *242*, 5460–5466.

(23) Chilapakul, O.; Crooks, R. M. *Langmuir* **1993**, *9*, 884.

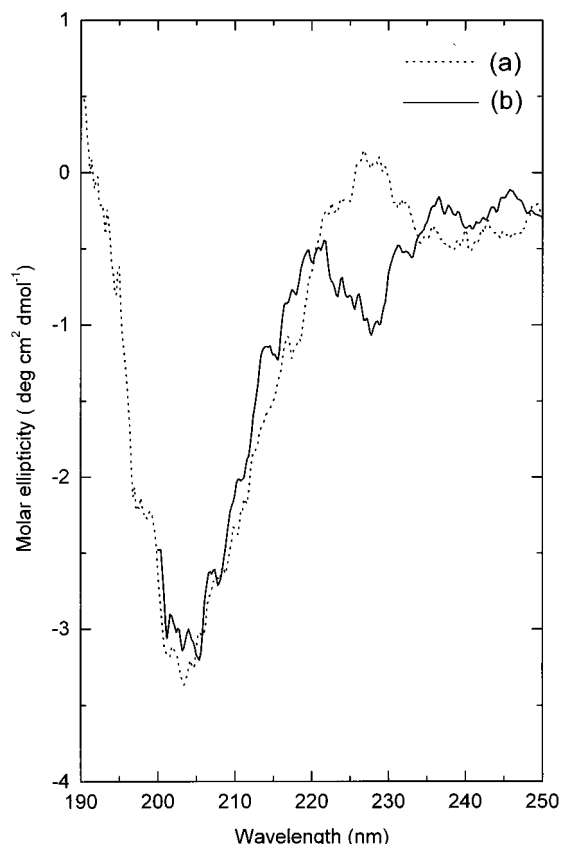


Figure 5. Electronic CD spectra of (a) indolicidin in water and (b) a PC vesicle (2 mM) with indolicidin (18 μ M). See text.

as was the case for the DPPA bilayer. One intriguing thing is that the amide bands in Figure 3d are about 1.7 times more intense than those in Figure 3b, suggesting that indolicidin molecules are incorporated more readily into the DPPC bilayer than into the DPPA bilayer. This may be due to the fact that the head group of DPPC is much bulkier than that of DPPA (*vide infra*).

We have previously suggested that the amide I band of indolicidin at 1664 cm^{-1} in Figure 2b could be due to either a random-coil or a 3_{10} - and/or distorted α -helical conformation. On the basis of the H/D exchange experiment, we ruled out the possibility of a random-coil structure. To get further information on the plausible conformation, a circular dichroism (CD) study was carried out.

Circular Dichroism Spectral Feature of Indolicidin in PC Vesicles. As mentioned in the Introduction, on the basis of a CD measurement, Falla et al.⁵ proposed that indolicidin should adopt a weak poly-L-proline II (PPII) extended helix structure inside POPC/POPG liposomes. Further, they concluded that the extended structure would span the membrane as an aggregate or be stacked in the membrane, since indolicidin should be too small to span the bilayer as an α -helix or β -strand. Ladokhin et al.⁶ reported, on the other hand, that indolicidin should adopt a slightly ordered but not an α -helical structure in SDS micelles. Besides, Yoder et al.²⁶ confirmed that a 3_{10} -helical conformation could be formed even from a peptide chain of five to six amino acid residues.

As shown in Figure 5, we have independently measured the CD spectra of indolicidin in the presence of PC vesicles. The spectral pattern of our CD spectrum is in fact very

similar to that of Ladokhin et al.⁶ taken in POPC and POPG vesicles. A weak negative band is observed at around 228 nm along with a strong negative band at about 205 nm.

Rabanal et al.²⁷ reported an overview of CD of proline-rich peptides. They demonstrated clearly that the PPII extended helix structure should be characterized by a weak positive peak at around 226 nm along with a strong negative peak at about 206 nm. On this ground, it can be supposed that indolicidin does not adopt a PPII helical structure inside the PC liposome. On the other hand, it has been documented in the literature^{28,29} that a right-handed 3_{10} -helical structure is characterized by a negative and fairly weak 225 nm band, followed by a strong negative 205 nm band and a weak positive band at about 195 nm. In fact, Yoder et al.²⁶ recently reported that right-handed β -bend ribbon spirals, a subtype of the 3_{10} -helical structure, were characterized similarly by a weak negative band at around 230 nm and a strong negative band at about 205 nm. By contrast, the spectrum of a right-handed α -helical structure^{28,30} is known to have two negative maxima at 222 and 208 nm with comparable high intensities and a very strong positive band near 195 nm. All of this information dictates that indolicidin should take a 3_{10} -helical conformation in PC vesicles.

One cannot rule out the possibility that indolicidin in the LB bilayers adopts a somewhat different conformation from that in unilamellar vesicles. Nonetheless, along with the present CD data, the fact that the main infrared absorption at 1664 cm^{-1} in Figure 3b and d matches well with the amide I band of a stable 3_{10} -helix strongly suggests that indolicidin molecules should be present as 3_{10} -helical conformers in DPPA, DPPC, and DPPG bilayers on ZnSe crystals. It should be pointed out that the amide I band observed in this work (1664 cm^{-1}) is significantly different from that of a stable PPII helical structure; for poly(L-proline),³¹ a prototypical PPII helix, the amide I' band (after deuteration) appears at 1636 cm^{-1} in the free state and at 1641 cm^{-1} inside the lipid.

Proline is unique among the amino acids in that the end of the side chain is covalently bound to the preceding peptide bond nitrogen. This leaves the backbone at this point with no amide hydrogen, so that no hydrogen bonding is possible. The five-membered ring also imposes rigid constraints on the N-C α rotation. Accordingly, the PPII conformation is known to be the most preferable structure for the proline residues.³² On the other hand, despite the constraints imposed by the proline residue, a large diversity of forms is also observed frequently in proline-rich peptides and proteins. MacArthur and Thornton³³ studied the influence of proline residues on protein conformation referring to the X-ray crystallographic data from the Brookhaven Protein Data Bank. For the 963 proline residues, over 38% were found in loops or random coils, with 26% in helices (α or 3_{10}), 23% in turns, and 13% in β -strands; of the 1021 proline residues in the sample, 166 were found in α -helices and 96 in 3_{10} -helices. All the

(27) Rabanal, F.; Ludevid, M. D.; Pons, M.; Giralt, E. *Biopolymers* **1993**, *33*, 1019–1028.

(28) Manning, M. C.; Woody, R. W. *Biopolymers* **1991**, *31*, 569–586.

(29) Anderson, N. H.; Liu, Z.; Prickett, K. S. *FEBS Lett.* **1996**, *399*, 47–52.

(30) Beychok, S. In *Poly- α -Aminoacids*; Fasman, G. D., Ed.; Dekker, New York, 1967; pp 293–337.

(31) Cabiaux, V.; Agerberth, B.; Johansson, J.; Hombl, F.; Goormaghtigh, E.; Ruysschaert, J. *Eur. J. Biochem.* **1994**, *224*, 1019–1027.

(32) Cantor, C. R.; Schimmel, P. R. *Biophysical Chemistry, Part 1: The Conformation of Biological Macromolecules*; W. H. Freeman & Co.: San Francisco, 1980; pp 86–101.

(33) MacArthur, M. W.; Thornton, J. M. *J. Mol. Biol.* **1991**, *218*, 397–412.

(26) Yoder, G.; Keiderling, T. A.; Formaggio, F.; Crisma, M.; Toniolo, C. *Biopolymers* **1995**, *35*, 103–111.

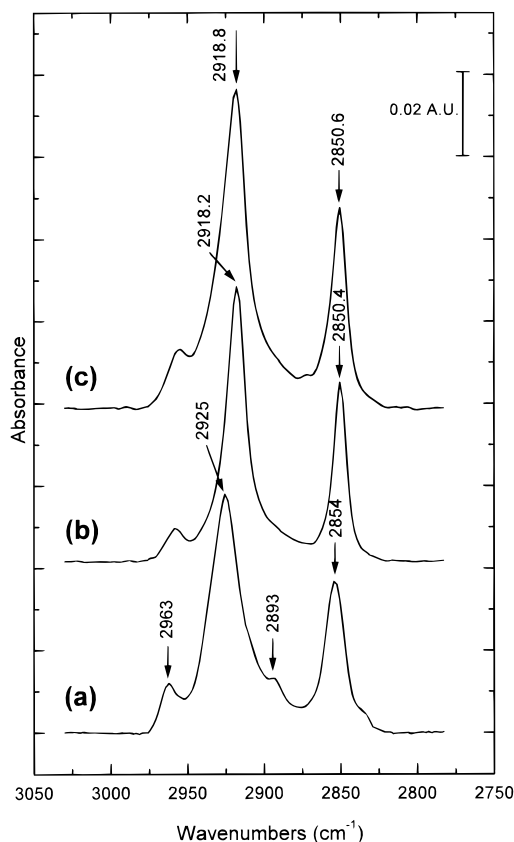


Figure 6. FTIR-ATR spectra in the C–H stretching region: (a) DPPA in CCl_4 ; LB films of DPPA bilayers on ZnSe (b) before and (c) after immersion in indolicidin solution ($50 \mu\text{g/mL}$) for 20 min.

proline residues in 3_{10} -helices were found, however, in the first turn, with the most favored location being the second position. Moreover, they claimed that the secondary structure of proline pairs separated by two or three other residues did not favor the helical conformation. In this sense, it is very intriguing that the CD and IR data obtained in this work dictate strongly that indolicidin should assume a 3_{10} -helical conformation not only in a neat state but also inside the model lipid bilayers. At the moment, it is not evident whether the usual interpretation of IR and CD data, based largely on correlation and regression of numerous protein data, is valid for the unusual tridecapeptide indolicidin.

ATR-IR C–H Stretching Bands of DPPA and DPPC after Interaction with Indolicidin. Figure 6a shows the ATR spectrum in the C–H stretching region for DPPA dissolved in CCl_4 . The peaks at 2925 and 2854 cm^{-1} can be assigned, respectively, to the antisymmetric and symmetric stretching vibrations of CH_2 groups.³⁴ The weak bands at 2963 and 2893 cm^{-1} can be assigned to the antisymmetric and symmetric stretching vibrations of CH_3 groups, respectively.³⁴ Figure 6b displays the ATR spectrum of a DPPA bilayer anchored on a ZnSe crystal by the LB method. Subtle differences can be noticed between the spectra shown in Figure 6a and b. First of all, peak positions are slightly different between the two spectra; namely, in the latter spectrum, the $\nu_{\text{as}}(\text{CH}_2)$ and $\nu_{\text{s}}(\text{CH}_2)$ bands appear, respectively, at 2918.2 and 2850.4 cm^{-1} . The $\nu_{\text{as}}(\text{CH}_3)$ and $\nu_{\text{s}}(\text{CH}_3)$ bands, although weak,

appeared, respectively, at 2956 and 2872 cm^{-1} in Figure 6b. The relative peak intensities are also significantly different between the two spectra.

Since the $\nu_{\text{as}}(\text{CH}_2)$ and $\nu_{\text{s}}(\text{CH}_2)$ vibrations are both somewhat sensitive to the conformation of acyl chains,^{35,36} their peak positions have been used frequently in the determination of structures and phase changes in phospholipid systems.^{37–39} As a more close-packed trans zigzag structure is assumed, the frequencies of the above modes are known to red-shift; the number of gauche conformers increases along with the increase in wavenumbers and widths of the $\nu_{\text{as}}(\text{CH}_2)$ and $\nu_{\text{s}}(\text{CH}_2)$ bands. In this sense, the difference in the peak positions of the two spectra in Figure 6a and b can be understood. The peak positions in Figure 6b are in fact very close to those of well-ordered crystalline hydrocarbons. This suggests that the compressed DPPA film at the air–water interface has been transferred successfully to the ATR crystal without any significant structural distortion.

Figure 6c represents the ATR spectrum taken after the DPPA bilayer on ZnSe was immersed in an indolicidin solution for 20 min. The spectral change is not significant; the $\nu_{\text{as}}(\text{CH}_2)$ and $\nu_{\text{s}}(\text{CH}_2)$ modes blue-shifted only by 0.6 and 0.2 cm^{-1} , respectively, and their band widths increased, respectively, by 2.5 and 0.8 cm^{-1} (for each sample, the amounts of peak-shift and band-broadening were reproducible within 0.1 and 0.4 cm^{-1} , respectively, albeit the sample-to-sample variation was somewhat larger than those quoted here (see Table 2).

As shown in Table 2, the $\nu_{\text{as}}(\text{CH}_2)$ and $\nu_{\text{s}}(\text{CH}_2)$ modes of DPPC, appearing, respectively, at 2918.1 and 2850.2 cm^{-1} before immersing the bilayer into indolicidin solution, were observed at 2918.9 and 2850.9 cm^{-1} after immersion. Concurrently, their band widths were observed to increase by 3.5 and 0.4 cm^{-1} , respectively. The peak shift and the band broadening occurring in the DPPC bilayer were somewhat larger than those in the DPPA bilayer. Although the spectral change in the C–H stretching region looks overall rather insignificant, the present observation may suggest that the conformation of acyl chains in DPPC is affected more than that in DPPA by the incorporation of indolicidin molecules.

Conformational change would be evidenced also by the variation in dichroic ratios of the $\nu_{\text{as}}(\text{CH}_2)$ and $\nu_{\text{s}}(\text{CH}_2)$ bands. Dichroic ratios of the $\nu_{\text{as}}(\text{CH}_2)$ and $\nu_{\text{s}}(\text{CH}_2)$ modes, defined as $R = A_p/A_s$, in which A_p and A_s are the absorbances measured, respectively, with p- and s-polarized light, are included in Table 2. Although not distinct, dichroic ratios change upon the interaction of lipid bilayers with indolicidin, and the change in DPPC is far greater than that in DPPA. It may be also worthwhile to note that the dichroic ratios of the $\nu_{\text{as}}(\text{CH}_2)$ and $\nu_{\text{s}}(\text{CH}_2)$ modes of the lipid bilayers were barely affected by the rotation of the ATR crystal; after 90° rotation, the R values of DPPA bilayers varied less than 0.02. Assuming that the acyl chains possess an extended trans zigzag conformation, the present observation suggests that the LB lipid bilayers can be described in terms of a uniaxial orientational model,^{40–42} in which transition moments are

(36) Li, M.; Rice, S. A. *J. Chem. Phys.* **1996**, *104*, 6860–6876.

(37) Buontempo, J. T.; Rice, S. A. *J. Chem. Phys.* **1993**, *98*, 5835–5846.

(38) Chollet, P.; Messier, J.; Rosilio, C. *J. Chem. Phys.* **1976**, *64*, 1042–1050.

(39) Moore, D. J.; Wyrwa, M.; Reboulleau, C. P.; Mendelsohn, R. *Biochemistry* **1993**, *32*, 6281–6287.

(40) Okamura, E.; Umemura, J.; Takenaka, T. *Biochim. Biophys. Acta* **1985**, *812*, 139–146.

(41) Ahn, D. J.; Franses, E. I. *J. Phys. Chem.* **1992**, *96*, 9952–9959.

(34) MacPhail, R. A.; Strauss, H. L.; Snyder, R. G. *J. Phys. Chem.* **1984**, *88*, 334–341.

(35) Mitchell, M. L.; Dluhy, R. A. *J. Am. Chem. Soc.* **1988**, *110*, 712–718.

Table 2. FTIR-ATR Peak Positions, Band Widths, and Dichroic Ratios of Symmetric and Antisymmetric Stretching Bands of CH₂ Groups in LB lipid Bilayers^{a,b}

sample	peak position ^c		band width ^d ($\Delta\nu$)		dichroic ratio ^d (R)	
	$\nu_s(\text{CH}_2)$	$\nu_{as}(\text{CH}_2)$	$\Delta\nu_s(\text{CH}_2)$	$\Delta\nu_{as}(\text{CH}_2)$	R_{2850}	R_{2918}
DPPA ^e	2850.4	2918.2	9.1 (± 0.3)	17.3 (± 1.3)	0.85 (± 0.01)	0.87 (± 0.01)
DPPA/indolicidin ^f	2850.6	2918.8	9.9 (± 0.1)	19.8 (± 1.1)	0.89 (± 0.02)	0.92 (± 0.02)
DPPC	2850.2	2918.1	9.8 (± 0.1)	17.3 (± 1.8)	0.81 (± 0.04)	0.84 (± 0.05)
DPPC/indolicidin	2850.9	2918.9	10.2 (± 0.4)	20.8 (± 1.9)	0.89 (± 0.01)	0.98 (± 0.01)

^a See text. ^b In cm^{-1} . ^c Regardless of the sample, peak position was reproducible within 0.1 cm^{-1} . ^d Values in parentheses represent uncertainties comprising the sample-to-sample variation. ^e See Figure 5b. ^f See Figure 5c.

assumed to be uniaxially distributed around the direction normal to the film surface.

The head group of DPPC is much bulkier than that of DPPA. This can be evidenced by the π - A isotherm shown in Figure 1. One can thus imagine that the acyl chains in DPPA bilayers are packed more closely than those in DPPC bilayers; the interchain space in the latter is larger than that in the former. This may allow the indolicidin molecules to be incorporated more easily into the DPPC bilayers than into the DPPA bilayers, so that the amide bands in Figure 3d appear more distinctly than those in Figure 3b (vide supra). Besides the size difference, the head group of DPPA (and DPPG) is negatively charged while that of DPPC is neutral. Considering that indolicidin is composed of positively charged amphiphilic peptides, at least in the initial stage, indolicidin will electrostatically interact more strongly with DPPA than with DPPC bilayers. It was concluded earlier that indolicidin resides inside the acyl chains of DPPA and DPPC bilayers. This may imply that the electrostatic interaction is not crucial for indolicidin to be incorporated into the lipid bilayers. Considering that the N-terminus of indolicidin has highly hydrophobic residues,⁴³ that is, Ile and Leu, their hydrophobic interaction with the possibly exposed acyl chains of lipid molecules would be more important than their electrostatic interaction.^{44–46}

ATR-IR Amide Bands of Indolicidin after Casting a DPPC/Indolicidin Mixture on ZnSe. ATR spectral patterns of the cast films of DPPA (or DPPG)/indolicidin mixtures were barely different from those of the LB films of DPPA (or DPPG) immersed in indolicidin solution. Supposing that, in the cast films, DPPA (or DPPG) molecules will form multi-bilayers, the present observation suggests that the hydrophobic interaction is more important than the electrostatic interaction between the DPPA (or DPPG) and the indolicidin molecules.

It was rather surprising to observe that the ATR spectral patterns of the cast films of DPPC/indolicidin mixtures were significantly different from those of the LB films of DPPC immersed in indolicidin solution. As shown in Figure 7a, the most intense amide I band was observed at 1687 cm^{-1} for the cast film, along with shoulder peaks at 1664 and $\sim 1640 \text{ cm}^{-1}$. The band at 1687 cm^{-1} can be attributed to a β -turn structure stabilized, as in a 3_{10} -helix, by the usual $1 \leftarrow 4$ intramolecular $\text{N}-\text{H} \cdots \text{O}=\text{CH}$ hydrogen bonds.^{21,47,48} A very similar infrared spectral pattern was also observed from the cast films of POPC/indolicidin mixtures, as can be seen in Figure 7b and c. Compared with the case for the DPPC/indolicidin film,

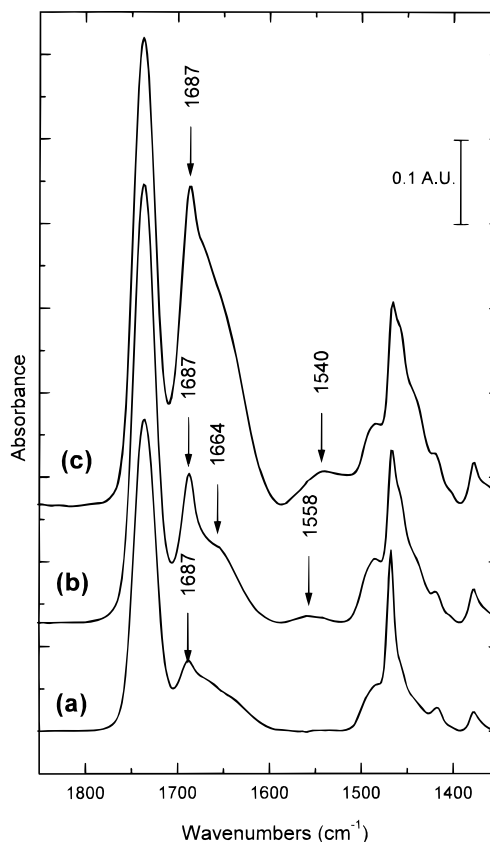


Figure 7. FTIR-ATR spectra in the $1400\text{--}1800 \text{ cm}^{-1}$ region; cast films of mixtures of (a) 30:1 (molar ratio) DPPC/indolicidin, (b) 30:1 POPC/indolicidin, and (c) 10:1 POPC/indolicidin on ZnSe.

the band assignable to a β -turn structure is stronger in the POPC/indolicidin film. Furthermore, the band became more distinct at a higher POPC/indolicidin molar ratio.

The different observations made of the cast films of DPPA/indolicidin and DPPC/indolicidin mixtures are quite intriguing. The origin of such differences can not be clarified at the moment. Nonetheless, the present observation clearly indicates that a 3_{10} -helical conformation should be more favorable for indolicidin inside the DPPA (or DPPG) bilayer than inside the DPPC bilayer.

Conclusion

We have examined the interaction of indolicidin, a tridecapeptide known to possess an antimicrobial activity, with model lipid bilayers, DPPA, DPPG, and DPPC, using FTIR-ATR spectroscopy. Along with the CV measurement, indolicidin molecules were found to be incorporated inside the acyl chains of the lipid bilayers upon coming into contact with LB lipid bilayers. In accordance with the CD measurement, it was concluded that indolicidin, consisting of an ill-defined random-coil structure in an aqueous medium, adopts a 3_{10} -helical conformation in LB lipid bilayers. A very similar conformation was found in

(42) Fringeli, U. P.; Schadt, M.; Rihak, P.; Gnthard, H. H. *Z. Naturforsch.* **1976**, *31a*, 1098–1107.

(43) Jacobs, R. E.; White, S. H. *Biochemistry* **1989**, *28*, 3421–3437.

(44) Yoon, B. J.; Lenhoff, A. M. *J. Phys. Chem.* **1992**, *96*, 3130–3134.

(45) Roth, C. M.; Lenhoff, A. M. *Langmuir* **1993**, *9*, 962–972.

(46) Roth, C. M.; Lenhoff, A. M. *Langmuir* **1995**, *11*, 3500–3509.

(47) Bandekar, J.; Krimm, S. *Proc. Natl. Acad. Sci. U.S.A.* **1979**, *76*, 774–777.

(48) Krimm, S.; Bandekar, J. *Biopolymers* **1980**, *19*, 1–20.

the cast films of DPPA/indolicidin and DPPG/indolicidin but a β -turn-like structure appeared to form more dominantly when a DPPC/indolicidin mixture was cast on an ATR substrate. The 3_{10} -helical conformation thus appeared to more favorably occur for indolicidin inside the DPPA (DPPG) bilayer than in the DPPC bilayer.

Finally, we have to mention briefly a few unexpected experimental observations. Namely, it was very intriguing that the perturbation of C–H stretching bands of model lipid molecules was not substantial even though indolicidin molecules were incorporated clearly inside the lipid bilayers. At the moment, its exact origin is not certain. The lack of real evidence of substantial lipid/peptide interaction may be caused by peptide aggregation, as found before for other peptides.^{49,50} Regarding this matter, we plan to do quartz crystal microbalance (QCM) and atomic force microscopy (AFM) studies; in-situ QCM and AFM studies will be performed in indolicidin solution by using a gold-coated quartz substrate covered with ODT and DPPA (or DPPC) monolayers and a mica substrate covered

with model DPPA (or DPPC) single bilayers, respectively. The QCM study is expected to reveal how many indolicidin molecules will be incorporated inside the lipid bilayer. The AFM study is expected to reveal the size of the aggregate that indolicidin molecules should form upon incorporation into the lipid bilayer. Besides, we hope a X-ray crystallographic study of indolicidin will be possible in the near future, since the indolicidin molecule, quite rich in proline, is supposed at a first glance not to be compatible with the 3_{10} -helical structure.

Acknowledgment. This work was supported in part by the Korea Research Foundation through the Non Directed Research Fund (1995), by the Korea Science and Engineering Foundation through the Specified Research Fund (95-0501-09) and the Center for Molecular Catalysis at Seoul National University (1997), and by the Ministry of Education, Republic of Korea, through the Basic Science Research Fund (1997). The authors acknowledge Prof. Byong-Seok Choi in the Korea Advanced Institute of Science and Technology for arranging for N.J.C. to use the CD spectrometer.

LA9708750

(49) Brauner, J. W.; Mendelsohn, R.; Prendergast, F. G. *Biochemistry* **1987**, *26*, 8151–8158.

(50) Jackson, M.; Mantsch, H. H.; Spencer, J. H. *Biochemistry* **1992**, *31*, 7289–7293.